Precursor route synthesis and thermal contraction of compounds $ZrW_{2-x}Mo_xO_8$ ($x = 0, 0.4, 0.6, 0.8, 1.2, 1.6$)

ZHANG, Shan-Ying[a](张山鹰) ZHAO, Xin-Hua*,[a](赵新华) MA, Hui[b](马辉)
WU, Xin-You[c](吴辛友)

[a] *Department of Chemistry, Beijing Normal University, Beijing 100875, China*
[b] *Analyzing and Testing Center, Beijing Normal University, Beijing 100875, China*
[c] *National Center of Analysis (Testing for Non-ferrous Metals & Electronic Materials, Beijing General Research Institute for Non-ferrous Metals, Beijing 100088, China*

A series of title compounds as well as their precursors were synthesized by precursor route. Their PXRD patterns were characterized with ZrW_2O_8 or $ZrMo_2O_8$ model by Rietveld method. The thermal contractions of the compounds were determined according to the variable-temperature PXRD data and NTE coefficients were presented. The two-phase mixture of $ZrW_{0.4}Mo_{1.6}O_8$ was also analyzed individually.

Keyword Thermal contraction, precursor route, $ZrW_{2-x}Mo_xO_8$

Introduction

Thermal contract compounds refer to a kind of compounds with average negative thermal expansion (NTE) coefficients of linear or of volume expansion over certain temperature range.[1,2] The compounds are the more important constituents of composite materials to control the very low thermal expansion coefficient and perhaps effect the physical properties of the materials such as dielectric behavior, refraction index, *etc*. A series of new functional materials for circuit board, optical substrates and other applied areas may be developed.

Cubic zirconium tungstate compounds (AW_2O_8, A = Zr, Hf) have recently received considerable attention since they undergo isotropic NTE behavior over a very broad temperature range as from 0.3 K to 1050 K.[3] It is considered that the property resulted from the unique structural characteristic.[4]

$ZrMo_2O_8$ is analogous to ZrW_2O_8 in structure. It reveals that cubic $ZrMo_2O_8$ can be achieved as a metastable phase under strict preparation conditions and is an analogy with β-ZrW_2O_8 both in structure and NTE property.[5] Meanwhile, ZrW_2O_8 related to trigonal $ZrMo_2O_8$ structurally has been prepared by nonhydrolytic sol-gel chemistry.[6] It possesses a positive thermal expansion property. ZrW_2O_8 and the Mo-substituted ZrW_2O_8 were prepared using low-temperature synthesis.[7] The effect of substitution of Mo for W lowers the α- to β-phase transition temperature. And it was reported that $ZrW_{1.6}Mo_{0.4}O_8$ is also a NTE compound.[7] But the other composition ($x = 0.7$—1.5) phases of the solid solution have not indexed completely because the extra phase occurs probably. In this paper, the Mo-substituted ZrW_2O_8 phases as well as the W-substituted $ZrMo_2O_8$ phases were indexed structurally and thermal expansion properties were studied without exception.

Experimental

Precursors $ZrW_{2-x}Mo_xO_7(OH)_2\cdot(H_2O)_2$ ($x = 0$, 0.4, 0.6, 0.8, 1.2, 1.6) were prepared using the starting materials ($Na_2WO_4\cdot 2H_2O$ (AR), $Na_2MoO_4\cdot 2H_2O$ (AR) and $ZrOCl_2\cdot 8H_2O$ (AR) were mixed stoichiometrically) in strong acidic aqueous solution at reflux temperature according to Ref. 8. Then they were dehy-

* Received November 30, 1999; accepted February 18, 2000.
Project (No. 29871006) supported by the National Natural Science Foundation of China.

drated at 423 K and the amorphous products were crystallized as $ZrW_{2-x}Mo_xO_8$ ($x = 0, 0.4, 0.6, 0.8, 1.2, 1.6$) crystals at 833 K. The dehydrated samples ($x = 0$, 0.4, 0.6, 0.8, 1.2) are of single phases, but the sample ($x = 1.6$) is a two-phase mixture.

The composition of title compounds was characterized using base melted-sulfocyanide spectrophotometric and ICP-AES methods. The weight-loss percentage of H_2O in precursors determined by thermogravimetric analysis corresponds to the calculated one of the formula $ZrW_{2-x}Mo_xO_8 \cdot 3H_2O$. The crystals were characterized by powder x-ray diffraction (PXRD). The PXRD data were recorded using step scan mode with 0.02°(2θ) step size from 10—120° for the hydrated compounds and 30° to 120° for the dehydrated compounds. Cu K_α radiation and Ni filter were used, and the step time was prolonged to 4 seconds. The *in situ* diffraction data at different temperatures were achieved on Rigako Dmax-3A equipped with high-temperature attachment. A type of K thermocouple situated next to the sample rack read samples' temperature.

The general structure analysis software GSAS[9] was used to refine patterns of $ZrW_{2-x}Mo_xO_7(OH)_2 \cdot (H_2O)_2$ ($x = 0$, 0.4, 0.6, 0.8, 1.2) and $ZrW_{2-x}Mo_xO_8$ ($x = 0$, 0.4, 1.2 and 1.6). Si was used as an internal standard for $ZrW_{2-x}Mo_xO_8$ ($x = 0$, 0.4, 1.2 and 1.6). Their lattice parameters at different temperature were refined from variable temperature PXRD data. The refinements were performed by fixing the lattice parameter of the internal standard of Si to be 0.543049 nm (293 K), 0.543124 nm (343 K), 0.543192 nm (383 K), 0.543363 nm (473 K), 0.543667 nm (623 K) and 0.543996 nm (773 K), which were deduced from its thermal expansion coefficients ($\times 10^{-6}$ K^{-1}) (2.5 (293 K), 2.9 (350 K), 3.2 (400 K), 3.5 (500 K), 3.8 (600 K), 4.0 (700 K) and 4.1 (800 K) for Si.[10]). The zero point parameter of the instrument as well as some profile variables were correction terms in refinements.

Results and discussion

Room temperature structure

The PXRD patterns of the precursors, $ZrW_{2-x}Mo_xO_7(OH)_2 \cdot (H_2O)_2$ ($x = 0, 0.4, 0.6, 0.8, 1.2$), were refined using $ZrMo_2O_7(OH)_2 \cdot (H_2O)_2$ (S. G. $I4_1cd$)[8] as the model. Then the ZrW_2O_8 was the starting model[3] for refinements of $ZrW_{2-x}Mo_xO_8$ ($x = 0$, 0.4, 1.2). The models were modified by substitution of Mo randomly according to their compositions. The all cell parameters and the details of the refinements are listed in Table 1 for $ZrW_{2-x}Mo_xO_7(OH)_2 \cdot (H_2O)_2$ ($x = 0, 0.4, 0.6, 0.8, 1.2$) and Table 2 for $ZrW_{2-x}Mo_xO_8$ ($x = 0$, 0.4, 1.2), respectively. Final observed, calculated plots and their differences of PXRD patterns of $ZrW_{1.6}Mo_{0.4}O_7(OH)_2 \cdot (H_2O)_2$ and that of $ZrW_{1.6}Mo_{0.4}O_8$, as representative examples for precursors and title compounds, are demonstrated in Fig. 1 and Fig. 2 (a).

Table 1 Refinement results of $ZrW_{2-x}Mo_xO_7(OH)_2 \cdot (H_2O)_2$ ($x = 0$, 0.4, 0.6, 0.8, 1.2) at room temperature

X	0	0.4	0.6	0.8	1.2
a (nm)	1.14515(4)[1.145][a]	1.14435(5)	1.14507(6)	1.14497(4)	1.14563(4)
c (nm)	1.24871(7)[1.249][a]	1.24791(8)	1.24791(8)	1.24895(7)	1.24979(6)
R_P (%)	9.57	8.61	8.15	8.59	9.45
R_{wP} (%)	12.90	10.94	10.15	10.83	11.99

[a] Refer to Ref. 11.

Fig. 1 shows that all reflections of precursors' patterns were indexed and refined by the model. The R_p reduced less than 10% means that the single phase was obtained. The fact that the occupancy of Mo substituted by W is sensitive to the quality of the refinement (R_p, R_{wp}) indicates that $ZrW_{2-x}Mo_xO_7(OH)_2 \cdot (H_2O)_2$ and $ZrMo_2O_7(OH)_2 \cdot (H_2O)_2$ are isomorphous.

In rich-W region, $ZrW_{1.6}Mo_{0.4}O_8$ possesses α-ZrW_2O_8 structure (S. G.: $P2_13$) at room temperature, which is similar to ZrW_2O_8. On the contrary, $ZrW_{0.8}Mo_{1.2}O_8$ at room temperature has β-ZrW_2O_8 structure (S. G.: $Pa\bar{3}$), which is a high temperature modification. This verifies that Mo-substitution for W lowers the phase transition temperature.

Table 2 Refinement rsults of $ZrW_{2-x}Mo_xO_8$ ($x = 0, 0.4, 1.2$) at different temperatures

T (K)		293	343	383	473	623	773
ZrW_2O_8	S.G.	$P2_13$	$P2_13$	$P2_13$	$Pa\bar{3}$	$Pa\bar{3}$	$Pa\bar{3}$
	a (nm)	0.91492(9)	0.91463(6)	0.91457(8)	0.91369(5)	0.91296(5)	0.91266(7)
	R_P (%)	10.91	10.96	10.29	9.92	9.80	10.74
	R_{wP} (%)	14.07	14.19	13.14	12.60	12.51	13.70
$ZrW_{1.6}Mo_{0.4}O_8$	S.G.	$P2_13$	$P2_13$	$Pa\bar{3}$	$Pa\bar{3}$	$Pa\bar{3}$	$Pa\bar{3}$
	a (nm)	0.91450(4)	0.91462(3)	0.91389(4)	0.91364(7)	0.91305(3)	0.91229(3)
	R_P (%)	11.24	11.28	10.05	10.35	9.82	10.39
	R_{wP} (%)	14.15	14.25	12.82	13.10	12.50	13.10
$ZrW_{0.8}Mo_{1.2}O_8$	S.G.	$Pa\bar{3}$	$Pa\bar{3}$	$Pa\bar{3}$	$Pa\bar{3}$	$Pa\bar{3}$	$Pa\bar{3}$
	a (nm)	0.91302(4)	0.91331(3)	0.91325(4)	0.91273(3)	0.91209(4)	0.91184(4)
	R_P (%)	10.95	10.63	10.37	11.05	11.09	10.70
	R_{wP} (%)	13.80	13.38	13.10	13.86	13.89	13.50

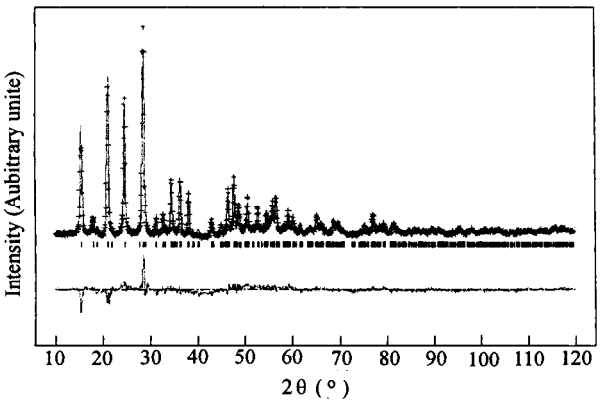

Fig. 1 PXRD patterns of the observed (+), calculated (−) plots, and their difference (lower) for $ZrW_{1.6}Mo_{0.4}O_7(OH)_2 \cdot (H_2O)_2$ at room temperature. Reflection positions are indicated by tick marks.

The PXRD pattern of the two - phase mixture $ZrW_{0.4}Mo_{1.6}O_8$ was refined with double phases of cubic β-$ZrMo_2O_8$ and trigonal $ZrMo_2O_8$ as the structural models in which their atomic site occupancies of Mo were modified randomly according to Mo: W = 0.8:0.2. Lattice parameters and mole ratios of the two phases were also refined. Final observed, calculated plots and their difference of $ZrW_{0.4}Mo_{1.6}O_8$ are shown in Fig. 3, and refinement details of $ZrW_{0.4}Mo_{1.6}O_8$ are listed in Table 3. As mentioned above, the metastable cubic β-$ZrMo_2O_8$ and trigonal ZrW_2O_8 were synthesized in a strict condition and nonhydrolytic sol-gel method, respectively. However, the two-phase mixture of cubic β-$ZrW_{0.4}Mo_{1.6}O_8$ and trigonal $ZrW_{0.4}Mo_{1.6}O_8$ phases is prepared in precursor route conveniently. The samples were naturally cooled in Muffle ovens instead of quench hot after being heated.

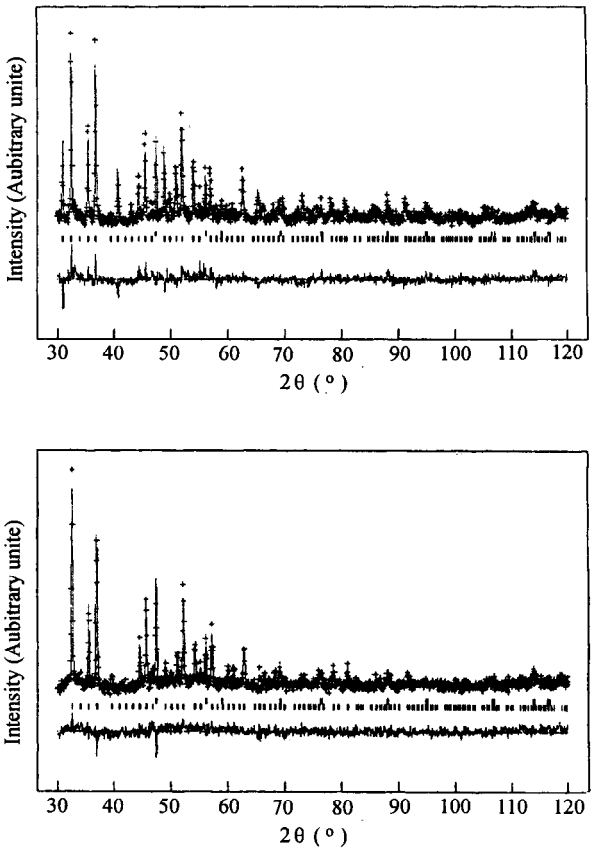

Fig. 2 PXRD patterns of the observed (+), calculated (−) plots, and a difference (lower) for $ZrW_{1.6}Mo_{0.4}O_8$ and internal standard (a) at room temperature and (b) 773 K. Reflection positions are indicated by tick marks (upper for internal standard and lower for $ZrW_{1.6}Mo_{0.4}O_8$).

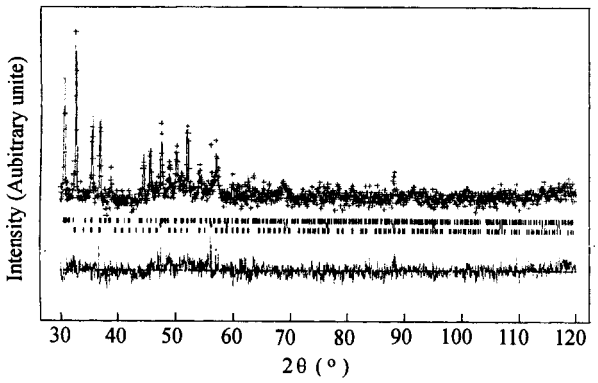

Fig. 3 PXRD patterns of the observed (+), calculated (-) plots, and their difference (lower) for $ZrW_{0.4}Mo_{1.6}O_8$ and internal standard at room temperature. Reflection positions are indicated by tick marks (upper for trigonal and lower for cubic phases of $ZrW_{0.4}Mo_{1.6}O_8$, middle for internal standard).

Thermal contract properties of the compounds

The cell parameters for $ZrW_{2-x}Mo_xO_8$ ($x = 0, 0.4, 1.2$) at different temperature were refined by Rietveld method. The refinements were performed with α-ZrW_2O_8 (space group: $P2_13$) for low temperature phase and β-ZrW_2O_8 (space group: $Pa\bar{3}$) for high temperature phase as the model. Fig.2(b) shows the refinement profile and difference of the sample ($x = 0.4$) of $ZrW_{2-x}Mo_xO_8$ ($x = 0, 0.4, 1.2$) at 773 K. The refinement results are listed in Table 2 and the depression of the phase transition temperatures for the compounds is related to Mo contents as shown in Table 2.

The dependence of cell parameters on temperatures about $ZrW_{2-x}Mo_xO_8$ ($x = 0, 0.4, 1.2$) is shown in Fig. 4. The average thermal expansion coefficient α_m of ZrW_2O_8 was calculated to be -5×10^{-6} K^{-1} from 293 to 773 K, as well as $ZrW_{1.6}Mo_{0.4}O_8$ and $ZrW_{0.8}Mo_{1.2}O_8$ to be -6×10^{-6} K^{-1} and -4×10^{-6} K^{-1} from 343 to 773 K, respectively (α_m defined as $(a_{t2} - a_{t1})/[a_{t1} \times (T_2 - T_1)]$).[3]

However, there was no phase transition when two-phase mixture $ZrW_{0.4}Mo_{1.6}O_8$ was heated to high temperature. Lattice parameters and mole ratio of the individual phase in the mixture were also refined in different temperature successfully. It is predictable that cubic phase possesses the thermal contract property and trigonal phase has the positive thermal expansion property for $ZrW_{0.4}Mo_{1.6}O_8$ as presented in Table 3.

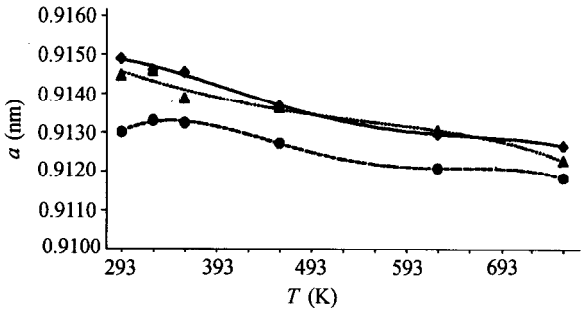

Fig. 4 Dependence of cell parameters (a) of $ZrW_{2-x}Mo_xO_8$ on temperature (T) ($x = 0$: ♦; $x = 0.4$: ▲; $x = 1.2$: ●).

Table 3 Refinement details of $ZrW_{0.4}Mo_{1.6}O_8$ at different temperatures

T (K)		298	343	383	473	623	773
R_p (%)		10.67	10.57	10.43	10.72	10.20	10.39
R_{wp} (%)		13.55	13.33	13.12	13.46	12.93	13.17
Cubic (S.G.: $Pa\bar{3}$)	a (nm)	0.91337(6) 0.91304(2)[a]	0.91333(5)	0.91334(4)	0.91302(5)	0.91221(4)	0.91157(5)
	V $(nm)^3$	0.761976	0.761873	0.761900	0.761085	0.759080	0.757485
	Mole ratio	0.8	0.8	0.8	0.8	0.7	0.7
Trigonal (S.G.: $Pa\bar{3}1c$)	a (nm)	1.0132(2) 1.01319(6)[b]	1.0138(2)	1.0143(2)	1.0139(1)	1.0135(1)	1.0121(9)
	c (nm)	1.1704(4) 1.17084(8)[b]	1.1754(5)	1.1770(3)	1.1858(2)	1.1979(2)	1.2042(1)
	V $(nm)^3$	1.040642	1.046236	1.048581	1.055585	1.065656	1.068159
	Mole ratio	0.2	0.2	0.2	0.2	0.3	0.3

[a] Refer to Ref. 5; [b] Refer to Ref. 12.

The volume expansion coefficients of cubic ($\alpha_{v\ Cubic}$) and trigonal ($\alpha_{v\ Trigonal}$) phases of $ZrW_{0.4}Mo_{1.6}O_8$ between 298—343 K and 383—773 K range (α_v defined as $(V_2 - V_1) / [V_1 - (T_2 - T_1)]$)[11] were calculated from the PXRD data and were displayed in Fig. 5. Furthermore, the thermal expansion preperty of the two-phase mixture can be estimated (see Table 4) by assuming that the coefficient of thermal expansion has an additive property in loose powders: $\alpha_c = \sum \alpha_i v_i$,[11] where α_c is the volume expansion coefficient of composite and α_i is that of the individual (listed in Table 4); v_i is the volume fraction of the ith component in the two-phase mixture, which was deduced from the mole ratio of the refinement results.

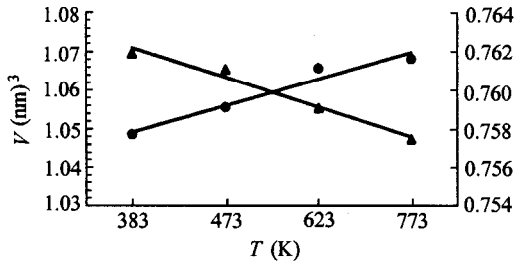

Fig. 5 The dependence of cell-volume (V) on temperature (T) for cubic (▲, right scale) and trigonal (●, left scale) phases in $ZrW_{0.4}Mo_{1.6}O_8$.

Table 4 Volume expansion coefficients of $ZrW_{0.4}Mo_{1.6}O_8$

Temperature range (K)	298—343	383—773
$\alpha_{v\ Trigonal}$ (K^{-1})	1.2×10^{-4}	4.8×10^{-5}
$\alpha_{v\ Cubic}$ (K^{-1})	-3.0×10^{-6}	-1.5×10^{-5}
$\alpha_{v\ two\text{-}phase}$ (K^{-1})	2.9×10^{-5}	1.2×10^{-7}

The results suggest a possibility to obtain materials with controlable thermal expansion coefficient by adjusting the mole ratio between cubic and trigonal phases. It is reasonable that Mo substituted for W content controls the phase ratio in the compound at room temperature.

References

1. Sleight, A.W., *Endeavour*, **19**, 64(1995).
2. Zhao, X.H., *HuaXue TongBao*, **11**, 19(1998).
3. Marry, T.A.; Evans, J.S.O.; Vogt, T.; Sleight, A.W., *Science*, **272**, 90(1996).
4. Evans, J.S.O.; Mary, T.A.; Subbramanian M.A.; Sleight, A.W., *Chem. Mater.*, **8**, 2809(1996).
5. Lind, C.; Wilkinson, A.P.; Hu, Z.B.; Short, S.; Jorgensen, J.D., *Chem. Mater.*, **10**, 2335(1998).
6. Wilkinson, A.P.; Lind, C.; Pattanaik, S., *Chem. Mater.*, **11**, 101(1999).
7. Closmann, C.; Sleight, A.W., *J. Solid State Chem.*, **139**, 424(1998).
8. Clearfield, A.; Blessing, R.H., *J. Inorg. Nucl. Chem.*, **34**, 2643(1972).
9. Larson, A.C.; Dreele, V.; Lansce, R.B., *Los Alamos National Lab*, Los Alamos, NM, 1994.
10. Liang, J.K., *Diagrams and Their Structures*, Scientific Press, Beijing, 1993, p.568-571.
11. Clearfield A.; Blessing, R.H., *J. Inorg. Nucl. Chem.*, **36**, 1174(1974).
12. Auray, M.; Quarton, M.; Tarte, P., *Acta Cryst.*, **C 42**, 257(1986).

(E9911166 JIANG, X.H.; DONG, L.J.)